

## Deposition of Cu and Ru Thin Films in Deep Nanotrenches/Holes Using Supercritical Carbon Dioxide

Eiichi KONDOH\*

*Interdisciplinary Graduate School of Medicine and Engineering, Department of Mechanical System Engineering, University of Yamanashi, 4-3-11 Takeda, Kofu 400-8511, Japan*

(Received November 26, 2003; accepted March 1, 2004; published June 29, 2004)

Supercritical CO<sub>2</sub> behaves like both a gas and a liquid, and possesses unique features such as nanopenetration capability, high diffusivity, and solvent ability. The technique described in this paper uses the supercritical CO<sub>2</sub> as a reaction medium for thin film growth and realizes filling or coating of nanofeatures with conducting metals. In this paper, we demonstrate the possibilities of this technique in Cu and Ru thin film deposition. A basic approach to achieving Cu metallization of deca-nanometer trenches or vias were studied. Ru, a promising material for capacitor electrodes and also a new candidate for the next-generation Cu barrier, was successfully deposited and its deposition characteristics were studied. Filling capability and the possibility of conformal deposition were also demonstrated as well as the fabrication of a Cu/Ru stack.

[DOI: 10.1143/JJAP.43.3928]

KEYWORDS: supercritical fluids, thin film deposition, copper, ruthenium

### 1. Introduction

Various deposition techniques are currently applicable for thin film growth in microelectronics applications. Physical vapor deposition (PVD), such as sputtering and evaporation, is the most common, and chemical vapor deposition (CVD) is also widely used. Electrochemical deposition (ECD) is a traditional technique for forming rather thick films, whereby solid thin films are formed from a liquid (electrolyte).

CO<sub>2</sub> transforms into a supercritical fluid above its critical point ( $P_c = 7.4$  MPa and  $T_c = 31^\circ\text{C}$ ).<sup>1)</sup> Supercritical CO<sub>2</sub> (scCO<sub>2</sub>) is a compressive fluid and behaves like both a gas and a liquid. ScCO<sub>2</sub> has so far been successfully utilized in chemical processing, such as for the extraction of fragrant materials, and is now of considerable interest for application to microprocessing. Advantageous characteristics of the scCO<sub>2</sub> fluid in view of microprocessing are, for instance, 1) a wide controllability of molecular number density, reaching as high as that of liquids, as functions of operating temperature and pressure, 2) high diffusivity and low viscosity, allowing deep penetration into small features, 3) zero surface tension and complete evaporation, which results in perfect wetting and drying without capillary force, 4) good solvating capability, allowing its use as an alternative to organic solvents, and 5) ease of design of an environmentally friendly closed-loop system. In addition, CO<sub>2</sub> is affordable and nonhazardous, and its critical point is low. The reported applications of scCO<sub>2</sub> for microelectronic processing include photoresist drying,<sup>2,3)</sup> precision cleaning,<sup>4-6)</sup> and the fabrication of porous low-dielectric-constant thin films.<sup>7,8)</sup>

Thin film deposition from scCO<sub>2</sub> fluids, frequently called supercritical fluid chemical deposition, has been reported.<sup>9,10)</sup> In this technique, metalorganic compounds (chelates), the precursors, are dissolved in scCO<sub>2</sub> and are transformed into thin films through an appropriate reaction chemistry. The film deposition from scCO<sub>2</sub> has so far been studied mainly from an academic point of view. However, impartially speaking, most of the work seems to have resulted in poor film quality compared to existing deposition techniques.

Metal filling of small features and conformal deposition onto a convexoconcave topography have always been of concern in ULSI metallization processes from interconnect fabrication to capacitor electrode formation. Pioneering research in using scCO<sub>2</sub> for ULSI metallization has been undertaken independently,<sup>11,12)</sup> proving that this technique meets the basic requirements for ULSI application, such as deep via/trench filling capability, deposition of (111)-preferential and low-resistivity films, and a high growth rate.<sup>13-15)</sup> Obviously, more work is needed to understand the deposition science and the pro and cons of this method in order to realize true ULSI processing.

We demonstrate the use of this technique for depositing metal thin films in deca-nanofeatures. Copper and ruthenium were chosen as the materials of study in this work because of their technological importance in ULSI metallization. Copper has been introduced in advanced integrated circuits as a replacement for conventional Al interconnects because of its lower bulk resistivity (1.55  $\mu\Omega$  versus 2.50  $\mu\Omega$  for Al).<sup>16)</sup> Ruthenium has received much attention as a promising capacitor electrode material, and is of concern as a next-generation barrier material in Cu metallization.

### 2. Experimental

A schematic diagram of the experimental setup is shown in Fig. 1. In the present experiments, a batch-type reaction system was used. The substrate (approx. 1 cm sq.) was placed in a stainless-steel reactor (approx. 2 ml) together with a predetermined amount of a precursor. The precursors used are shown in Fig. 2 and will be described later along with the formula. The reactor was then filled with H<sub>2</sub>, typically at 1 MPa, following reactor evacuation with a rotary pump. Liquid CO<sub>2</sub> was pumped using a plunger pump of a liquid chromatograph to attain a reaction pressure of 13 MPa. Finally, the reactor was heated to predetermined temperature. In this arrangement, the temperature at which the deposition reaction started may not be exactly determined. Therefore, when the temperature dependence of the growth rate was studied, a semi-batch arrangement was also employed, where the precursor was dissolved in the reservoir and then introduced to the substrate-containing reactor maintained at a constant temperature. Table I

\*E-mail address: kondoh@yamanashi.ac.jp

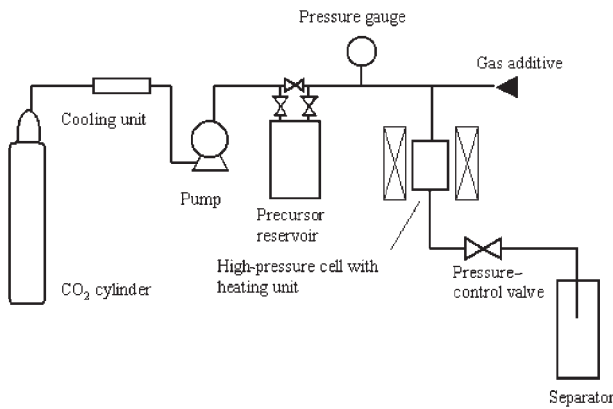


Fig. 1. A schematic diagram of experimental apparatus used in this work.

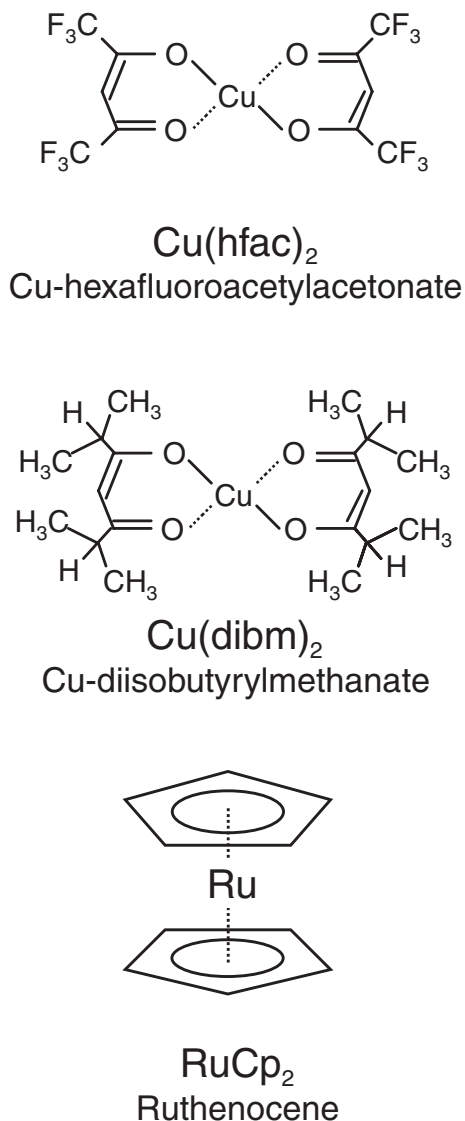


Fig. 2. Chemical structures of the precursors used in this study.  $\text{Cu}(\text{hfac})_2$ ,  $\text{Cu}(\text{dibm})_2$ , and  $\text{RuCp}_2$ .

summarizes the experimental conditions.

The substrates used were blanket or hole/trench-patterned  $\text{SiO}_2/\text{Si}$  wafers coated with atomic-layer-deposition (ALD) TiN, unless otherwise stated. The substrates were coated with Au using a conventional sputtering tool for electron

Table I. Growth conditions for supercritical fluid chemical deposition.

Precursors <sup>†</sup>	$\text{Cu}(\text{hfac})_2$ , $\text{Cu}(\text{dibm})_2$ , $\text{RuCp}_2$
Molar concentration	typ. $\approx 10^1$
Hydrogen partial pressure	1 MPa
Total pressure	13 MPa
Reactor Temperature <sup>†</sup>	180–400°C
Deposition time <sup>†</sup>	3–15 min
Substrates	Blanket or patterned ALD-TiN/SiO <sub>2</sub> /Si stacks

<sup>†</sup>see text.

micrography prior to the supercritical fluid deposition. The nominal thickness of the Au layer was about 50 Å. The deposited films were characterized using the JEOL JSM6500 field emission secondary electron microscope (SEM), Rigaku RAD1 X-ray diffractometer (XRD), Shimadzu ESCA750S or JEOL JPS9200 X-ray photoelectron spectroscope (XPS), and JEOL JAMP7810 Auger electron microprobe. XRD measurements were performed with a  $\theta$ - $2\theta$  arrangement, and XPS measurements were performed with a Mg  $K_\alpha$  X-ray source.

### 3. Results and Discussion

#### 3.1 Deposition of Cu and deca-nanofilling

The most fundamental experiment necessary to understand film deposition chemistry is the determination of the temperature dependence of growth. Film topography in narrow features is generally a trade-off between mass transport and the reaction proceeding inside. Therefore, better understanding of deposition chemistry is crucial for the improvement of film topography. Note that there has been no such systematic study reported so far on supercritical fluid chemical deposition, to the extent of the authors' knowledge.

Cu started to be deposited at around 180°C when the semi-batch reaction system (see above) was employed with hexafluoroacetylacetonatecopper ( $\text{Cu}(\text{hfac})_2$ ) as a precursor (hfac = hexafluoroacetyl-acetonate). This is much lower than typical CVD temperatures observed under  $\text{Cu}(\text{hfac})_2 + \text{H}_2$  chemistry.<sup>17)</sup> A preferential growth on conductive substances, including refractory metals such as Fe, Au, Cu, WN, TiN, TaN and HF-treated p-Si was observed without the Au coating. When the Au coating was applied, no deposition selectivity was observed. Without the Au coating, the deposition starting temperature increased by several tens of °C. The logarithmic deposition rate plotted against the reciprocal temperature is shown in Fig. 3.<sup>14,15)</sup> The deposition time was fixed at 15 min for all experiments. The film thickness shows a maximum at around 220°C and then decreased with increasing temperature. The activation energy for deposition was evaluated to be 0.42 eV. This value is almost one-half of the values reported for CVD and is approximately the same as that for plasma-assisted CVD (Table II<sup>18–20)</sup>).

A low CVD starting temperature and a low activation energy were reported when  $\text{Cu}(\text{hfac})_2$  was delivered as a solution in isopropanol.<sup>17)</sup> Despite the similarity of the use of a solvent, the critical difference from the present work is its role. Isopropanol serves as the reduction agent for deposition. On the contrary,  $\text{CO}_2$  is chemically inert and is not a

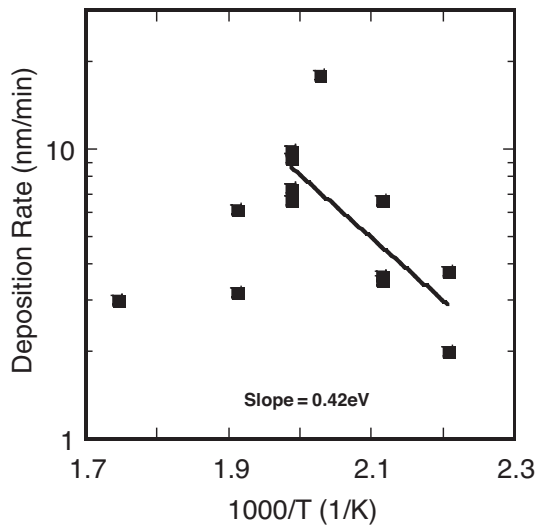


Fig. 3. Arrhenius plot of Cu deposition from scCO<sub>2</sub> fluid.

Table II. Activation energies for Cu film growth using Cu(hfac)<sub>2</sub>.

This work	Thermal CVD	Plasma CVD
0.42	0.65	0.39

strong proton donor even in the supercritical state. Obviously, solvation in scCO<sub>2</sub> played an important role in promoting the deposition reaction.

Such differences in deposition chemistry are thought to greatly effect the deposition topography. Figure 4 shows cross-sectional SEM images of Cu films deposited in narrow trenches using Cu(hfac)<sub>2</sub>. The films formed in larger trenches show smooth and conformal topography. The size of the smallest trenches seen in Fig. 4 is about 50 nm at the

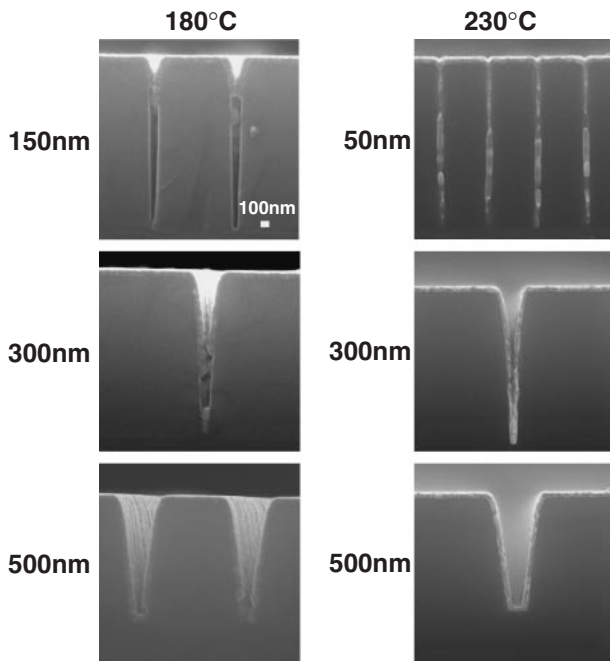


Fig. 4. Cross-sectional SEM images of films deposited using Cu(hfac)<sub>2</sub>. The nominal dimension is defined as the trench width at the opening. The magnification is the same in all micrographs.

opening. Cu plugged in these trenches at 230°C was continuous and showed no clear seams.

An interesting feature to stress here is that lowering the temperature from 230°C to 180°C was ineffective in improving the film conformability. For instance, Cu did not reach inside the trenches where the trench sealing occurred. A better Cu penetration is seen for the larger trenches; however, a discontinuity is still seen at the sidewall. This tendency is contrary to the general belief in CVD to occur where the conformability improves as the deposition temperature decreases.

The trench/via filling capability was found to also depend on the kind of precursor. When fluorine-free diisobutrylmethanatecopper (Cu(dibm)<sub>2</sub>, dibm = diisobutrylmethanate. See Fig. 2) was used instead of Cu(hfac)<sub>2</sub>, a significant improvement in deep via filling was achieved under the same deposition conditions (Fig. 5). The deposition temperature was 230°C in both experiments. The increase in temperature resulted in poorer filling in the deposition using Cu(hfac)<sub>2</sub> but in no significant effect on that using Cu(dibm)<sub>2</sub> (Fig. 6).

The reason for obtaining better filling in the Cu(dibm)<sub>2</sub> experiment is not clear at present. Thermal analyses of the precursors show much higher sublimation and decomposition temperatures of Cu(dibm)<sub>2</sub> than those of Cu(hfac)<sub>2</sub>.<sup>21)</sup> The higher decomposition temperature suggests a lower deposition rate at the same deposition temperature and thus better filling, as long as the CVD theory is valid. However,

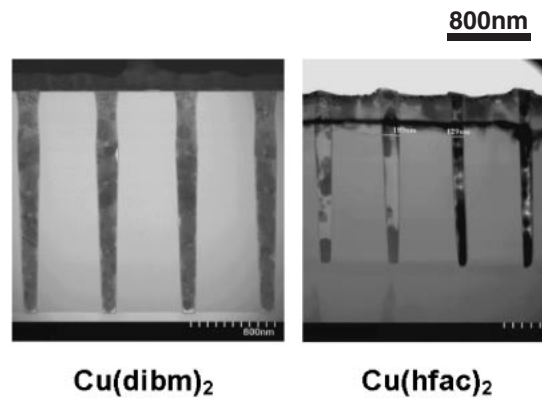


Fig. 5. Cross-sectional TEM images of 190 nm Cu vias using Cu(dibm)<sub>2</sub> (left) and Cu(hfac)<sub>2</sub>. The magnification is the same for both.

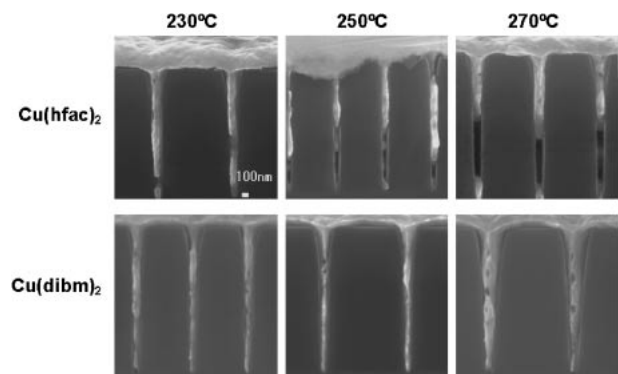


Fig. 6. SEM images of films deposited using Cu(hfac)<sub>2</sub> (above) and Cu(dibm)<sub>2</sub> (below). The magnification is the same in all micrographs.

as described above, lowering the temperature does not always lead to conformal topography or better filling. This topic is left as a future subject.

3.2 Ru deposition: deposition chemistry, filling and conformal deposition, and Cu barrier potential

One challenge in supercritical fluid metallization is barrier metal deposition. Recently, Ru has been proposed as a next-generation barrier metal against Cu diffusion.<sup>22)</sup> In addition to its low resistivity ( $6.67 \mu\Omega\cdot\text{cm}^{16}$ ), Ru is almost insoluble in Cu, has a high melting point of over  $2300^\circ\text{C}$ , and may be formed by CVD or be plated by electroless deposition.<sup>22,23)</sup> Moreover, Ru has received much attention as a promising capacitor material, because it has a low resistivity and etching capability, and its oxides are conductive. In view of deposition topography, fundamental requirements for the above applications are the same; namely good step coverage and filling capability. In the following, the characteristics of Ru deposition from supercritical  $\text{CO}_2$ , the first success deposition to the author's knowledge, are described and the possibility of the application to the Cu barrier metal is demonstrated.

The precursor used was bis(cyclopentadienyl)-ruthenium(II), (ruthenocene,  $\text{RuCp}_2$ ).  $\text{RuCp}_2$  is a yellow solid with a vapor pressure of about 0.01 Torr at  $85^\circ\text{C}$ .<sup>23)</sup> A preliminary experiment was carried out to study the solubility of  $\text{RuCp}_2$  in  $\text{scCO}_2$  using a high-pressure cell having view ports.  $\text{RuCp}_2$  dissolved well in  $\text{scCO}_2$  at 13 MPa and  $30\text{--}80^\circ\text{C}$  and became more soluble with increasing temperature. Although the solubilities of  $\text{RuCp}_2$  at higher temperatures have not been quantitatively documented, there is no doubt that the solubility considerably at much elevated temperatures, since the vapor pressure of  $\text{RuCp}_2$  has a large positive temperature dependence.

Deposition was carried out at  $250\text{--}350^\circ\text{C}$  and 13 MPa with the addition of  $\text{H}_2$ , as listed in Table I. The deposits obtained with the addition of  $\text{O}_2$  were granular or porous bulk. When  $\text{H}_2$  was used, the deposits became continuous metallic film. Figure 7 shows an XRD pattern of Ru film deposited at a furnace temperature of  $250^\circ\text{C}$ . The positions of pronounced 100, 002, and 101 peaks agreed well with those of the standard data sheet, as well as faint 102 and 103 peaks.

Figure 8 shows the result of AES depth analysis of a deposited Ru film. The signal from the Ru KLL band ( $\blacklozenge$ ) shows a typical depth profile of a single-element film. Signals of impurity elements are as low as the background

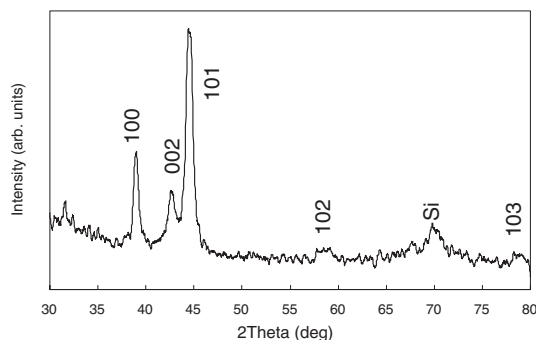


Fig. 7. XRD pattern of deposited Ru film.

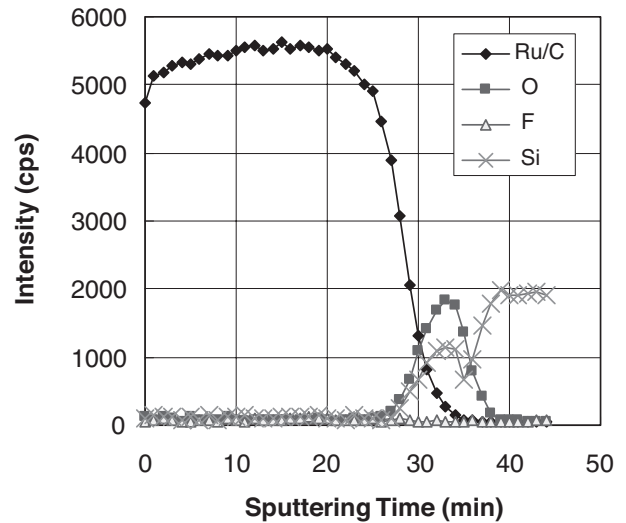


Fig. 8. AES depth profile of Ru film.

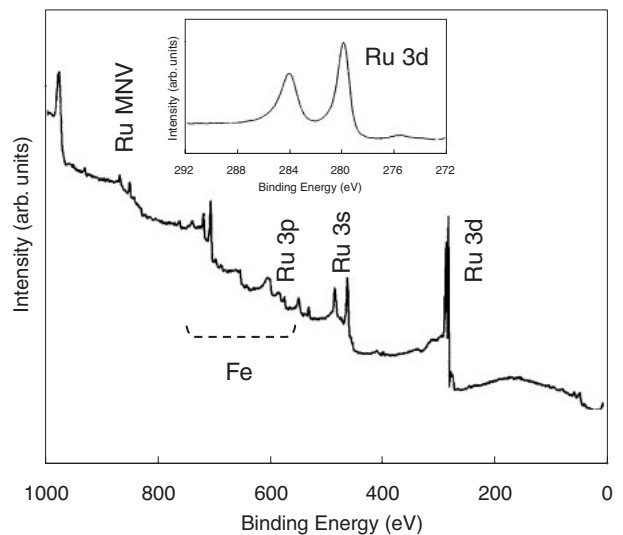


Fig. 9. XPS surface spectrum of Ru film. Fe peaks are attributed to the substrate holder.

signal. The signal from the Ru LMM band (not shown), of which the intensity is much weaker than those of the others, showed the same behavior as that of the Ru KLL. The C KLL band overlapped the Ru KLL band, thus the C impurity was not easily detectable. An XPS surface spectrum obtained after Ar surface sputtering clearly indicates the presence of strong Ru peaks and no impurity C or O (Fig. 9).

Figure 10 shows cross-sectional SEM images of an on-trial Cu/Ru stack (right) and a thin conformal Ru film (left). The Ru film in the right has a thickness of about 50 nm and shows very smooth and continuous topography. The Cu film in the left was also formed in  $\text{scCO}_2$  using  $\text{Cu}(\text{hfac})_2$  following a different run for Ru deposition. The valley in Ru is filled with Cu to the bottom, and the Cu/Ru interface is very clear and sharp. Figure 11 shows an SEM image of trenches filled with Ru. The width of the trench bottom was about 100 nm and the aspect ratio was about 20. Filling of such narrow deep trenches is of practical importance for fabricating ULSI capacitors and may be applicable to other metallization vihecles. These micrographs clearly indicate



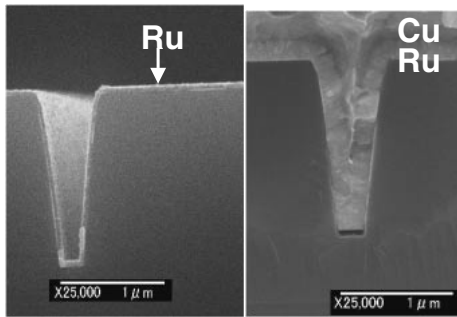


Fig. 10. Cross-sectional SEM images of a conformal 50-nm-thick Ru film (left) and a Cu/Ru stack (right). Note that Cu and Ru were formed in supercritical fluid.

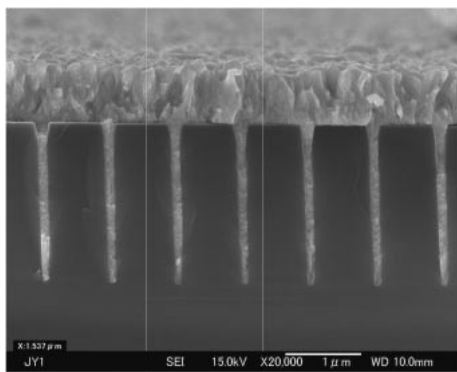


Fig. 11. Cross-sectional SEM images of 100 nm-at-bottom trenches filled with Ru. Vertical white lines in the middle are the scales for end-to-end measurements.

the vast potential of  $\text{scCO}_2$  deposition for true metallization.

Ru CVD using metalorganic precursors such as cyclopentadienyl-Ru ( $\text{RuCp}_2$ ) and Ru- $\beta$ -diketonates have received much attention for their capability to attain good conformal step coverage.  $\text{RuCp}_2$  has high chemical stability and high vapor pressure, and therefore, has been regarded as a promising precursor.<sup>23–25</sup> However, it has been reported that ruthenium films can be deposited from  $\text{RuCp}_2$  only under oxidative chemistry, or at least not under reducing chemistry. Green *et al.* reported, in their pioneering Ru metalorganic experiments, that no film growth was observed when  $\text{H}_2$  was conducted with vaporized  $\text{RuCp}_2$ . It has also been reported that Ru thin films were rarely grown from  $\text{RuCp}_2$  or its homologues either in inert gas or in vacuum ambient.<sup>23,25,26</sup>

The disagreement of the present results with the general belief concerning CVD suggests a critical difference in the deposition mechanism. From a practical point of view, the nonnecessity of  $\text{O}_2$  would ease the effort required to optimize the process conditions, because the residual oxygen greatly increases the film resistivity.

#### 4. Summary and Conclusion

We demonstrated the capability of a thin film deposition technique from supercritical  $\text{CO}_2$  fluids to fill/coat nano-features. In this technique, a metal precursor was dissolved in  $\text{scCO}_2$  and converted to a thin film through an appropriate reaction chemistry. A Cu deposition process has been developed, and filling/coating properties of Cu were found

to depend on the deposition temperature and the kind of precursor. Lowering the deposition temperature, which, in CVD, has been believed as an effective way of improving the conformability, did not result in better film coverage. The choice of precursor was also crucial, and using a low-vapor-pressure precursor led to a better performance for sub-100 nm trenches and holes. The deposition of Ru—a strong candidate material for capacitor electrodes and also for future-generation Cu barriers—from  $\text{scCO}_2$  using  $\text{RuCp}_2$  was reported for the first time, and the basic deposition characteristics were studied. The incorporation of  $\text{H}_2$  was necessary to obtain a continuous film; however  $\text{O}_2$  addition was not effective, contrary to general reported CVD procedures. Excellent filling and coverage performances were observed. In conclusion, supercritical fluid chemical deposition is a promising method for filling and coating of nano-features, and the underlying chemistries seem to be greatly different from those in CVD.

#### Acknowledgements

The author acknowledges K. Shigama, M. Hishikawa, and S. Sunada for their assistance in experiments, and V. Vezin for performing the STEM work. Part of this work is supported by a Grant-in-Aid for Scientific Research of the MEXT (*Monbu-Kagaku-Sho*), a Grant-in-Aid for Scientific Research from the Japan Society for the Promotion of Science, and by the Ministry of Economy, Trade, and Industry (METI) through New Energy and Industrial Technology Development Organization (NEDO).

- 1) R. Span and W. Wagner: *J. Phys. Chem. Ref. Data* **25** (1996) 1509.
- 2) H. Namatsu, K. Kurihara, M. Nagase, K. Iwadate and K. Muras: *Appl. Phys. Lett.* **66** (1995) 2655.
- 3) D. L. Goldfarb, J. J. de Pablo and P. F. Nealey: *J. Vac. Sci. & Technol. B* **18** (2000) 3313.
- 4) E. Bok, D. Kelch and K. S. Schumacher: *Solid-State Technol.* **35** (1992) 117.
- 5) G. L. Bakker and D. W. Hess: *J. Electrochem. Soc.* **145** (1998) 284.
- 6) C. W. Wang, R. T. Chang, W. K. Lin, R. D. Lin, M. T. Liang, J. F. Yang and J. B. Wang: *J. Electrochem. Soc.* **146** (1999) 3485.
- 7) S. V. Nitta, V. Pisupatti, A. Jain, P. C. Wayner, Jr., W. N. Gill and J. L. Plawsky: *J. Vac. Sci. & Technol. B* **17** (1999) 205.
- 8) N. Kawakami, Y. Fukumoto, T. Kinoshita, K. Suzuki and K.-i. Inoue: *Jpn. J. Appl. Phys.* **39** (2000) L182.
- 9) B. M. Hybertson, B. N. Hanse, R. M. Barkley and R. E. Sievers: *Mater. Res. Bull.* **26** (1991) 1127.
- 10) O. A. Louchev, V. K. Popov and E. N. Antonov: *J. Cryst. Growth* **155** (1995) 276.
- 11) E. Kondoh and H. Kato: *Microelectron. Eng.* **64** (2002) 495.
- 12) J. M. Blackburn, D. P. Long, A. Cabañas and J. J. Watkins: *Science* **294** (2001) 141.
- 13) E. Kondoh: *Proc. Advanced Metallization Conference 2002* (Material Research Society, PA, 2003) p. 463.
- 14) E. Kondoh, V. Vezin, K. Shigama, S. Sunada, K. Kubo and T. Ohta: *Proc. 2003 IEEE International Interconnect Technology Conference*, p. 141.
- 15) E. Kondoh and K. Shigama: *Proc. Advanced Metallization Conference 2003* (Material Research Society, PA, 2004) p. 583.
- 16) *CRC Handbook of Electrical Resistivities of Binary Metallic Alloys*, eds. K. Schröder (CRC Press, Boca Raton, 1983).
- 17) N. S. Borgharkar, G. L. Griffin, H. Fan and A. W. Maverick: *J. Electrochem. Soc.* **146** (1999) 1041.
- 18) D.-H. Kim, R. H. Wentorf and W. N. Gill: *J. Electrochem. Soc.* **140** (1993) 3267.
- 19) A. E. Kaloyeros and M. A. Fury: *Mater. Res. Bull.* **18** (1993) 22.
- 20) Y. D. Chen, A. Reisman, I. Turlik and D. Temple: *J. Electrochem.*

- Soc. **142** (1995) 3903.
- 21) Data sheets from material suppliers.
  - 22) O. Chyan, T. Arugagiri and T. Ponnuswamy: J. Electrochem. Soc. **150** (2003) C347.
  - 23) M. L. Green, M. E. Gross, L. E. Papa, K. J. Schnoes and D. Brasen: J. Electrochem. Soc. **132** (1985) 2677.
  - 24) T. Aoyama, M. Kiyotoshi, S. Yamazaki and K. Eguchi: Jpn. J. Appl. Phys. **38** (1999) 2194.
  - 25) S.-E. Park, H.-M. Kim, K.-B. Kim and S.-H. Min: J. Electrochem. Soc. **147** (2000) 203.
  - 26) Y. Matsui, M. Hiratani, T. Nabatame, Y. Shimamoto and S. Kimura: Electrochem. Solid-State Lett. **4** (2001) C9.